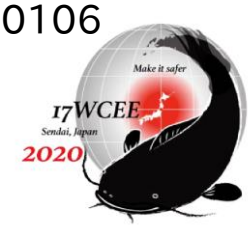

17th World Conference on Earthquake Engineering, 17WCEE
Sendai, Japan - September 13th to 18th 2020

Reinforced concrete beam producing re-centring and energy dissipation by yielding lower reinforcement prior to upper reinforcement

S. Shioya[(1)], A. Kawasoe[(2)]

[(1)] *Professor, Kagoshima University, shin@aae.kagoshima-u.ac.jp*
[(2)] *Professor, National institute of technology Kagoshima college, kawasoe@kagoshima-ct.ac.jp*

Abstract

New structural systems, minimizing damage during earthquakes and aftershocks for a quick reoccupancy, are desired. The key is to minimize maximum response displacement of building in earthquake and its residual displacement immediately after it. For reinforced concrete frame, techniques using pre-stressing have already been developed. However, the techniques require more cost than that of conventional reinforced concrete structure. It is useful and desirable that a device of arrangement and amount of reinforcements in beam can produce potential to minimize the residual displacement, like self-centring. The damage control almost means to control maximum response story drift angle of a building in earthquake. In general, the story angles to induce damages in finishing and equipment of buildings are smaller than those of structural members designed according to the current structural design code in Japan. The allowable story angle for finishing and equipment should be approximately 1.0-1.25%.
Therefore, criteria of the seismic design of buildings would be divided into three phases: no-damage in frequent-small earthquakes, the maximum story drift must be suppressed less than 0.5%; almost no-damage and no-residual displacement, irrespectively of yield of longitudinal reinforcements of beams or columns in Big-earthquake, the maximum drift must be less than 1.0-1.25%; and a certain of damage and residual displacement can be allowed in Mega-earthquake, assuring the life-safety of occupants.

The goal of this study is to develop design techniques to minimize residual displacement of buildings after the Big-earthquake for the second phase. We are finding potential to minimize the residual displacement of reinforced concrete frame buildings by controlling so that the amount of lower reinforcement is smaller than that of upper reinforcement of beam ends connected with column. This technique can produce shear force-displacement hysteresis loops to perform re-centring of building.

This paper introduces the concept of the technique and reports a loading experimental test of reinforced concrete beams to investigate its effectiveness for the re-centering.

Keywords: reinforced concrete structure; beam; moment frame; re-centring; damage control

1. Introduction

New structural systems, minimizing damage and residual displacement during earthquakes and aftershocks for a quick reoccupancy, are desired and several buildings have already been built based on the concept, where post-tensioning technologies developed for precast-concrete structure has been adopted[1,2,3]. The techniques have also been adopted to steel structure and timer engineering structure buildings[4-7]. Most of structural members of those structures are precast, and tensioning is added by the technology to interface to between the members to generate rocking on the interface. Moreover, dissipater devices are incorporated over the interface to reduce maximum response during earthquake and residual displacement after it. Recently, a friction-dumping device, which can produce self-centering with maintenance-free, has been developed[8].

However, in Japan, the technologies have been rarely adopted on the ground of inexperience and cost of the technologies and lack of understanding of the quick reoccupancy after earthquake. Pre-cast concrete and cast-in-place reinforced concrete buildings have been designed with conventional connections with reinforcement for general reinforced concrete building. One of best ways to spread the design to avoid damage and residual displacement for reinforced concrete buildings, is to improve low damage performance and re-centring potential by adjusting reinforcement for reinforced concrete building.

On the other hand, vibration-control structure for steel structure buildings usually minimize the residual displacement by restoring force of elastic frame. The system can avoid the residual displacement by adjusting the stiffness ratio of damping device to the frame and its damping force. One of characteristics of reinforced concrete members is to select amount, strength, and arrangement of reinforcements in one structural member. We have been developing reinforcement arrangement for beam of cast-in-place reinforced concrete frame to produce high re-cenetring performance, based on the concept of the vibration-control structure.

This paper reports detail of the reinforcement of beam, the mechanism of the recenering, and an experimental loading test of beams for verification of the concept. We have also investigated re-centering for column and rocking multi-storey shear wall yielded by beneding at bottom of first storey, and have recommended to re-centre frame by restoring force produced by gravity load, i.e., dead load and live load, regardless of yielding of longitudinal reinforcement in the column or the shear wall.

2. New beam-column connection

2.1 Reinforcement arrangement

Fig.1 illustrates an example of reinforcement arrangement for beam-column connection producing re-centring and energy dissipation. Upper reinforcement is high-strength steel deformed rebar; lower reinforcement is mild-steel deformed rebar. A certain length S at beam end of the reinforcements is debonded by wrapping with tape (like VM tape) in order to avoid concrete cracks accompanied by yielding of rebar there, and additional reinforcements are added to prevent cracks by moment which concrete there is subjected to.

As be mentioned in Section 3.2, decreasing amount of lower reinforcement can improve the performance of re-centering. In the case, the lower portion of concrete at the beam end can crush in compression when upper reinforcement is high-strength rebar and its amount is more than that of lower reinforcement. To avoid the crushing, No-tension reinforcements, which can resist only compression, are added. The No-tension reinforcement consists of three portion reabers and are bonded by light-pressure welded to ensure so that axes of the portion rebars coincide with, as shown in Fig.1(c). Detail of the weld work is mentioned in Section 3.1.

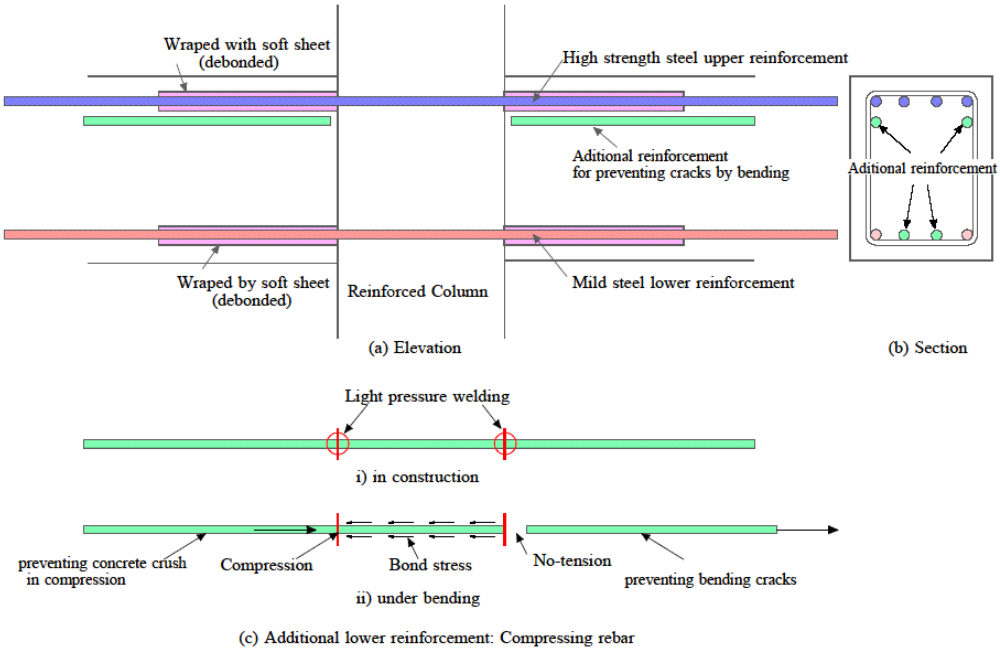

Fig. 1 – Reinforcement arrangement for beam-column connection producing re-centring potential

2.2 Elastic restoring force and its stiffness after lower reinforcement yielding

Vertical stiffness and capacity of beams after the lower reinforcement yielding varies depending on longitudinal reinforcement arrangement at beam ends. Fig.3 illustrates skeleton curves of vertical shear force and displacement relationship of the beams. The curves are based on assumption: the beam end sections are assumed as Fig.2 (a); rotation angles of both left-hand and right-hand beam ends are assumed to be equal; skeleton curves of stress-strain relationship of rebar are realized as shown Fig.2(c). Young's modulus of both

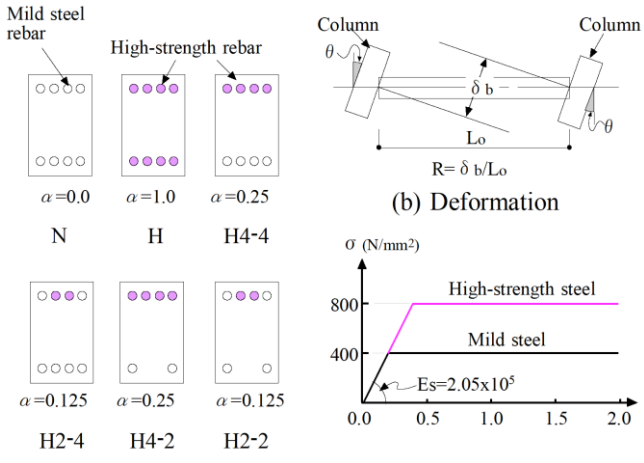

Fig. 2 – Rebar arrangement patterns for beam, configuration of derformation, and assumed stree-train cureve for rebars in tenion or compresion

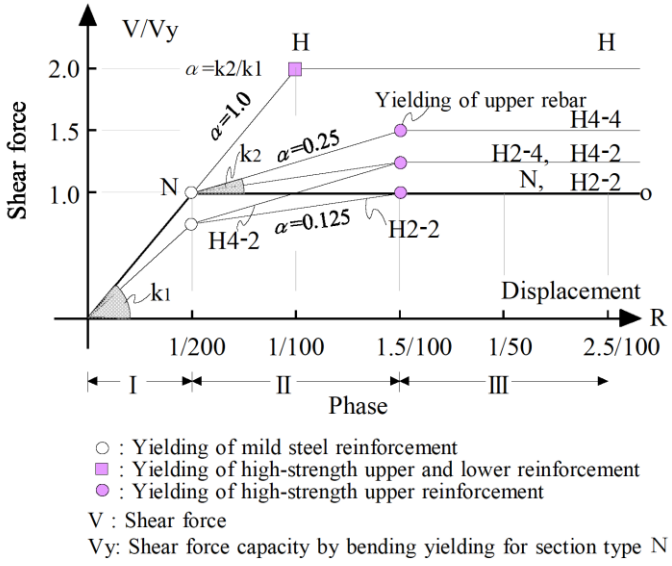

Fig. 3 – Predicted vertical shear force-displacemet skelton curves for beams with sections in Fig.1 and stiffness k1, k2

them is assumed to be same and yielding strength of high-strength steel is assumed to be twice of that of mild steel. Fig.4 shows curvature distributions of beam with section H4-4 in Fig.2(a). Fig.4(a) indicates the distribution at yielding of lower reinforcement; Fig.4(b) indicates increase of curvature after the yielding; Fig.4(c) indicates curvature distributions at yielding of high-strength upper reinforcement of right-hand beam end. Second stiffness after the first yielding can be mainly calculated as a cantilever in which the left-hand end is a pin and the right-hand end is a fixed end. The second stiffness k_2 can be estimated to be one quarter of the first stiffness k_1. The increase of shear force until high-strength upper reinforcement yield after the lower reinforcement yield is estimated one half of the increase for beam with section H in Fig.2(a). Elastic restoring force can be maintained by high-strength upper reinforcement until its yielding of right-hand section.

2.3 Amplification system for energy dissipation of lower reinforcement

Only lower reinforcement yields and dissipates energy until high-strength upper reinforcement yield of right-hand end for beam with section H4-4. Fig.5 illustrates curvature distribution at the high-strength upper reinforcement yielding, which indicates curvature except the left-hand hinge. Suppose that both rotation angle θ of beam-column nodes is equal, two angles calculated by integrating curvature over each range separated at inflection point of the beam should be equal. In Fig.5, the amount of curvature component of grey portion is suggested to concentrate into the left-hand plastic hinge. This mechanism boosts elongation of lower reinforcement of the left-hand end and its energy dissipation by the rocking.

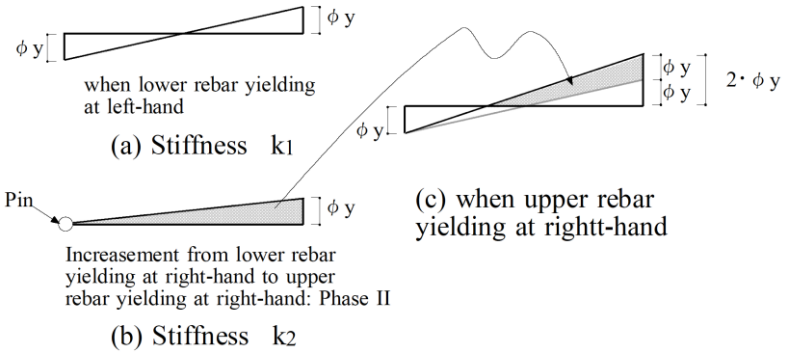

Fig. 4 – Curvature distribution patterns for stiffness k1, k2, and when upper rebar yielding at rightt-hand

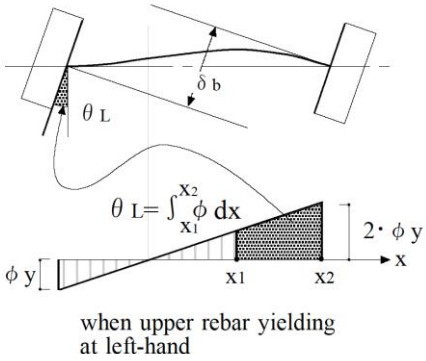

Fig. 5 – System of boosting elongation of lower reinfoecement for energy disspation

2.4 Deflection and moment of beam under long-term gravity load after earthquake

When bean ends in reinforced concrete flame yield during earthquake, bending stiffness of the ends decreases and the moment in the beam subjected to gravity load varies from those before the earthquake, as dash-line shown in Fig.6(b)[3]. The moment and deflection at mid-span of the beam may exceed allowable limits under long-term gravity load, whereas not-yield of upper reinforcement will prevent them from increasing, because bending stiffness of the ends rarely degrades under the long-term load after the Big-earthquake.

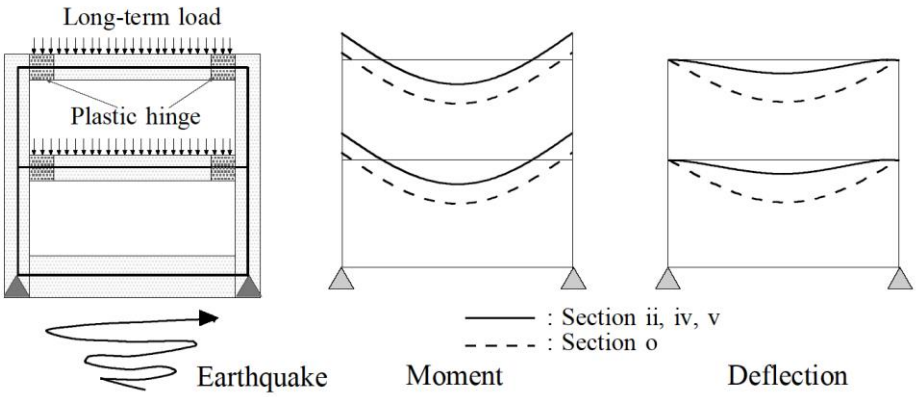

Fig. 6 – Variations of beam's moment and deflection corresponing to the sections after beam's plastic hinge yield during Big-earthquake

2.5 Effect of gravity moment on frame under short-term loading and system of suppressing column moment in frame during full mechanism during unexpected Mega-earthquake.

Fig.7 illustrates patterns of moment of a frame with beam section H4-2: Fig.7(a) indicates a pattern under long-term gravity loading; Fig.7(b), under gravity loading (GL) and short-term loading during an relative small or middle earthquake; Fig.7(c), under the GL and Big-earthquake; Fig.7(d), under unexpected Mega-earthquake. Although allowable moment of the left-hand beam end decreases by reducing the amount of lower reinforcement, moment of the ends under the GL, as Fig. 7(a), will mitigate the reduction of the allowable moment at the short-term loading as Fig.7(b). At right hand beam ends, high-strength upper reinforcement raises those allowable moment under short-term loading and sufficiently overcomes the increase of the ends due to GL. During expected Big-earthquake in design, assumed that the left-hand beam ends may yield and the right-hand beam ends not yield as Fig.7(c), re-centring of the frame can be expected to generate due to the upper reinforcements in elastic.

On the other hand, during unexpected Mega-earthquake in design, yield moment magnitude of right hand end increases due to the high-strength upper reinforcement. However, yield moment magnitude of the left hand ends is small due to mild-steel and small amount of its lower reinforcement, which is not-affected by moment under GL. Consequently, moment of beam-column node dose not increase so much.

For the frame with beam section H4-2, the increase is estimated to be approximately only 25 % of the magnitude of the fame with beam section O. This increase should be recognized as a compensation to produce re-centring potential in the frame.

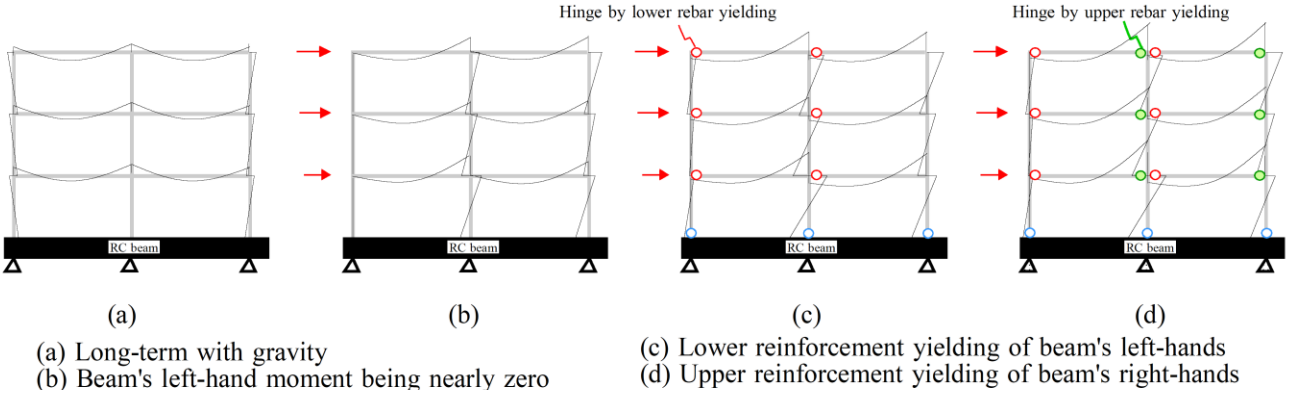

Fig. 7 — Schematic frame moment pattrns and yielding hinges as siesmic horizontal loads increasing

2.6 Assurance for re-centring system during Big-earthquake

Fig.8 illustrates vertical shear force-deformation curves for beam with high-strength steel upper reinforcement and mild steel lower reinforcement, when its deformation is configuration as Fig.2(b). Fig.8(a) indicates a skeleton curve for beam without mild-steel lower reinforcement. Fig.8(b) indicates a skeleton curve and hysteresis loops of beam including the effect of the mild-steel. Fig.8(c) indicates a skeleton curve and hysteresis loops by mild-steel lower reinforcement, obtained by subtracting shear force component of Fig.8(a) from that of Fig.8(b). The mild-steel rebars mean to be a dumping device with a certain rigidity.

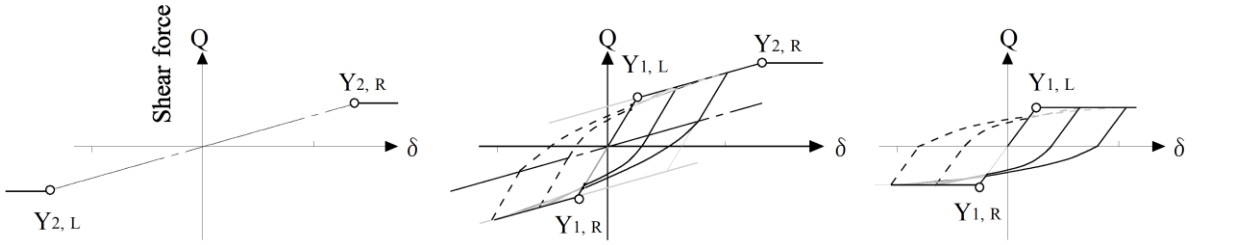

(a) Re-centring by high-strength reinforcement (b) Beam (c) Dissipation by lower reinforcement

Y_1 : Yielding of lower reinforcement, Y_2 : Yielding of upper reinforcement, L : Laft-hand connection , R : Rigth-hand

Fig. 8–Vertical shear force - deformation curves for beam with high-strength steel upper reinforcement and mild steel lower reinforcement, i.e., beam section H4-4 or H4-2

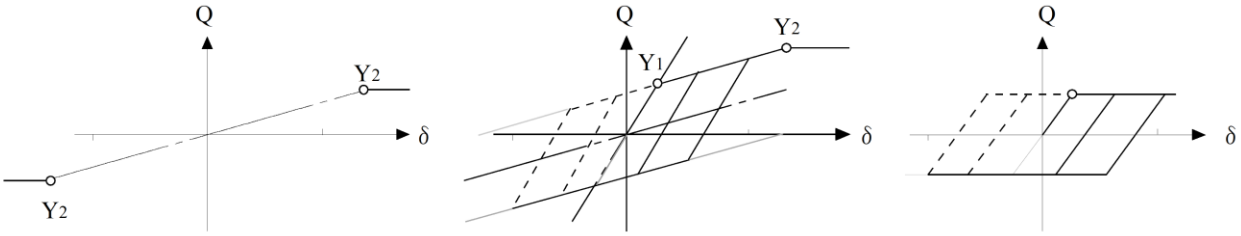

(a) Frame (b) frame with damper (c) Dissipation by damper

Y_1 : Yielding of damper device, Y_2 : Yielding of frame

Fig. 9 –Schematic horizontal force - deformation curves for vibration control framed structure

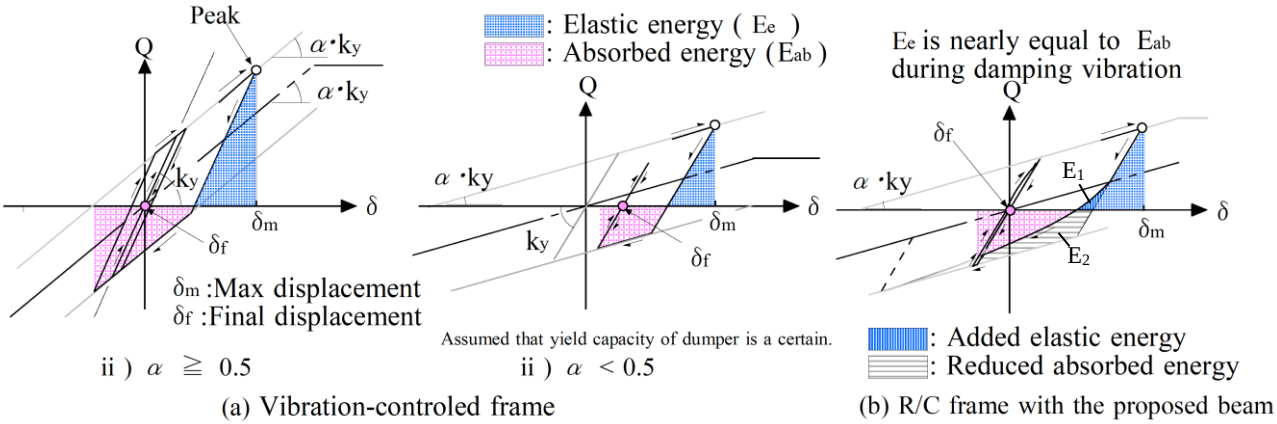

(a) Vibration-controled frame (b) R/C frame with the proposed beam

Fig. 10– Hysteresis loops and final residual displacement after free-vibration following maximum response for vibration controled frame and frame with proposed beams

On the other hand, vibration-control structure for steel structure buildings usually minimize the residual displacement by restoring force of elastic frame. The system can avoid the residual displacement by adjusting the stiffness ratio of damping device to the frame and its damping force. Fig.9 illustrates schematic horizontal force-deformation skeleton curve and hysteresis loops for vibration control framed structure. The frame with all beam producing the skeleton curve and hysteresis loops in Fig.9(b) can be expected to produce the skeleton curve and hysteresis loops similar to Fig.9(b) and minimize the residual displacement after Big-earthquake. The essential difference between Fig.7 and Fig.8 is configuration of loops of dumping device: the loops in Fig.8(c) is similar to Ramberg-Osgood rule; the loops in Fig.9(c) is similar to elastic-perfectly plastic rule.

For vibration-control structure frame, the residual displacement is minimized by selecting stiffness ratio of the second stiffness k_2 to the first stiffness k_1 and dumping force. In general, residual displacement after earthquakes for that frame is known to be less thang that of the frame converged by subjecting the frame to fee-vibration immediately after maximum response assumed in design.

Fig.10 illustrates hysteresis loops and final residual displacements after free-vibration following maximum response for vibration-controlled frame and frame with the proposed beam. Elastic energy Ee (blue area) released from the response peak to a point at force being zero is transferred to kinetic energy and next absorbed as elastic energy and plastic energy E_{ab} during reloading to negative direction. If its negative peak reach the negative skeleton curve, residual displacement converges to nearly zero with vibration dumping as Fig.10(a). Without completing the reach as shown in Fig.10(b), however, the residual displacement remains variable and uncertain after earthquake.

Fig.10(c) illustrates hysteresis loops for frame with the proposed beam producing loops in Fig8(c). Because the loop rule almost follows Ramberg-Osgood rule, the E_e (blue area) of its loop increases by vertical shaded area E_1; the absorbed energy E_{ab} in reloading to negative decreases by horizontal shaded area E_2, compared with Elastic fully plastic rule like Fig.9(c). The decrease of the shade energy facilitates the negative peak reaching easily to the skeleton curve and improves the re-cenetring of frame.

By selecting the stiffness ratio of k_2/k_1 and dumping force of the frame with the proposed beam, the residual displacement of the frame may be ensured to be minimized to nearly zero, as well as the vibration-controlled structure.

3. Exprimental verification

Experimental tests were carried out on reinforced concrete beams with high-strength upper reinforcement and lower mild-steel reinforcement. The aims were to: 1) study the magnitude of minimizing the residual displacement in relation to the vertical beam maximum displacement; 2) gain information on the ratio of the second stiffness to the first stiffness (the secant at yield of lower reinforcement) and max response limit displacement to ensure the re-centring of beam; and 3) investigate low damage of the beam with the deboned rebar as mentioned in Section 2.1.

3.1 Specimens

Four beam specimens scaled down at 1:4 were tested. Fig.11 illustrates configuration of the specimens and arrangement of reinforcements. Table 1 shows beam sections of the specimens, which employed two kind of pattern of H4-2 or H4-4 in Fig.2(a). H-No.1 was arranged two mild-steel rebars for lower reinforcement and four high-strength rebars for upper reinforcement; H-No.2 was arranged four mild-strength rebars for the lower and four high-strength rebars for the upper. N-No.1 was a control specimen for H-No.1; N-No.2 was for H-No.2, of which all reinforcements employed mild-steel rebars. At mid-span except beam ends in H-No.1 and N-No.1, four mild-steel rebars were arranged for lower reinforcement, considering to resist to long-term gravity moment in design.

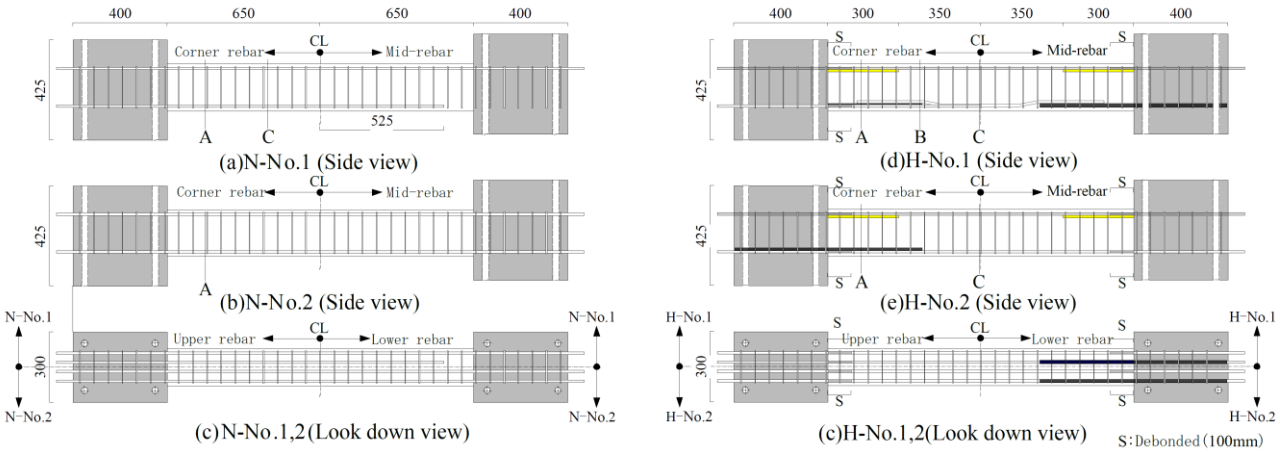

Fig. 11 – Reinforcement arrangement for beam specimensl

Table –1 Beam sections

Specimen	N-No.1	H-No.1		H-No.2	N-No.1	N-No.2	H-No.1	H-No.2
Section position	A	A	B	A	C	A	C	C
Section	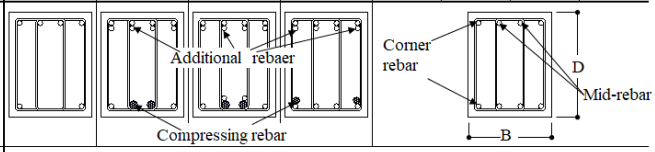							
Dimension	B:Beam width=160mm, D:Beam depth=200mm							
Upper rebar	4-D10	4-D10(H)			4-D10		4-D10(H)	
Additional rebar	—	4-D10			—			
Lower	2-D10		4-D10					
Compressing rebatr		2-D16		2-D13	—			
Stirrup	4-D3.5@60							

D10(H): High-strength steel rebar, Nominal diameter is 10mm

Table –2 Mechaniacl properties of materials

unit : N/mm^2

	Specimen	Ec ($\times 10^4$)	σ_B	ε_B(%)
Concrete	N,H-No.1	2.88	40.7	0.25
	N,H-No.2	2.92	49.5	0.27
	Diameter	Es ($\times 10^5$)	σ_Y	σ_P
Rebar	D10	1.80	383	—
	D10(H)	1.87	1085	820
	D13	1.83	380	—
	D16	1.81	366	—
	D3.5	2.05	385	—

Ec, Es : Young's modulus, σ_B : Compressive strength
ε_B (%) : Strain at σ_B, σ_Y : Tensile yield strength
σ_P : Tensile strength at proportional limit

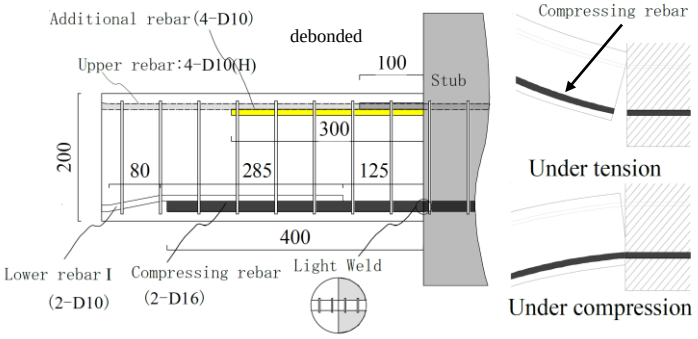

Fig. 12 – Compressing rebaer at lower of beam end to avoid cruch of concrete for H-No.1

The debonded length over rebar at beam ends of H-No.1 and H-No.2 was a half of beam depth, i.e., 100 mm; the debonded length was not applied to the control specimens. In order to avoid bending cracks over the debonded length and decay of plastic hinge at the beam end, mild-steel reinforcements were added to the ends. Fig.12 illustrates an example of reinforcements at the end of H-No.1. Crush of concrete may occur at the lower of beam ends under bending because upper reinforcements are a high-strength rebar. To avoid the crush, the additional reinforcement is a rebar jointed with three-cut rebars by light-pressure-welding, as mentioned in Section 2.1, which can resist under compression and not resist under tensile as shown in Fig.12 right. This rebar is herein referred to as “compressing rebar”. Tensile strength of separation of the welding portion in tensile test of employed compressing rebar was approximately 140N/mm^2 and the time of the press work was approximately 6.5seconds. In H-No.1, as the compressing rebars were interfered

with the mid-span lower reinforcement I mentioned above, the two reinforcements were folded as rebar-I shown in Fig.12. Shear reinforcement ratio was 0.40%. Table 2 shows mechanical properties of materials for the specimens.

3.2 Test setup

Fig.13 shows configuration of test setup for measuring displacements. Fig.14 shows configuration of test setup for loading. Two vertical forces were reversed-cyclic loading with increasing vertical displacement between the left-hand side stub and the right-hand stud, adjusting the rotation angles of both stubs to be equal, by the vertical two actuators. By the two vertical forces of the actuators, moment of beam ends can be calculated. Fig.16 shows protocol of target displacement with numbers of loading cycle. The displacements of positive peaks and negative peaks were chosen to be same. The loading was divided into the following three phases.

In the first phase, the target displacement angle i.e. drift was gradually increased up to 1/50rad.; immediately after reaching the each target drift, quasi-static reversed cyclic loadings (QRCLs) imitating free vibration, were conducted in order to investigate the re-centering ability of beam, assuming residual vibrations immediately after maximum response at Big earthquake.

In the second phase, the target drift was returned to 1/200rad., and the target was again gradually increased up to 1/50rad.; as well as the first phase, the residual vibration loading was applied after reaching each of the targets. This phase was conducted, assuming that building may experience two-time Big earthquakes.

In the third phase, the targets were assigned to drifts after 1/50rad., assuming unexpected Mega-earthquake, and reversed cyclic loadings were conducted until fracture.

Loading processes for the free-vibration after target displacement were applied, as the following to: increase the displacement δ_b (see Fig.5) between left column and right column until Es area equals E_e area in Fig.15, where E_s represents sum energy of elastic energy and plastic energy during reloading to negative direction, and E_e is sum energy released from the peak to point at force being zero; immediately after it, unload and reload to positive direction as the prior half amplitude; determine the final residual displacement converged by continuing these processes until following the elastic energy E_e converges to nearly zero.

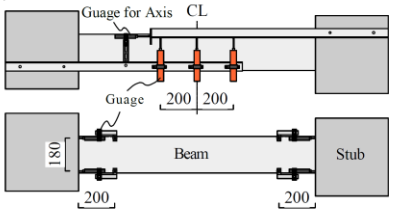

Fig. 13 – Set-up for dsiplacement

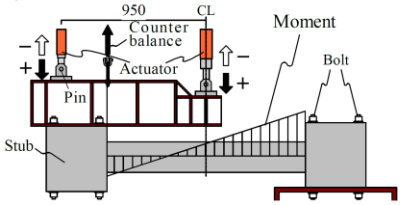

Fig. 14 – Set-up for loading

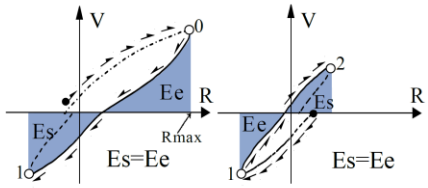

Fig. 15 – Free-vibration loading processes

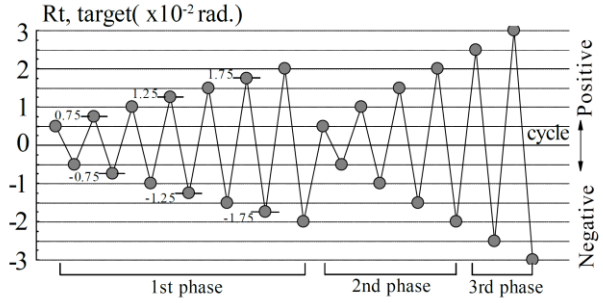

Fig. 16 – Fig. Target displacement protocol

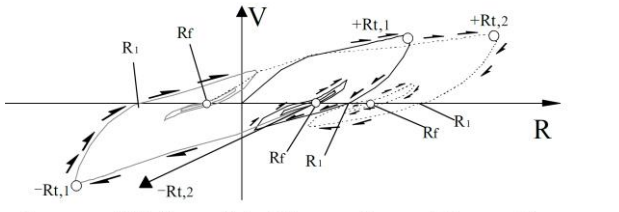

Fig.17 – Loading process for determining residual displacementafter quasi-staticfree-vibration

3.3 Results

3.3.1 Shear force-displacement curves and hysteresis loops

Fig.18 shows Vertical shear force-drift curves and hysteresis loops: Fig.18(a) is free-vibration hysteresis loops toward positive loading targets; Fig.18(b) is those toward negative peaks. Drift of vertical axis is angle by dividing the displacement δ_b by beam length L as shown in Fig.2(b). In the Fig.18, several events are indicated by marks. The ○ mark indicates final residual displacement converged after free-vibration loading.

Although, of the conventional beam specimens, i.e., N-No.1 and N-No.2, the final residual displacement have increased as target displacement increasing, of the proposed beam, i.e., H-No1 and H-No.2, the final displacements have converged to approximately zero in both positive and negative loading directions, in particular, those of H-No.1 are extremely near zero until starting of upper reinforcement yield.

Fig.19 plots drifts at events of yielding of reinforcements and crushing of concrete for the positive direction loading. The drifts of lower reinforcement yielding of N-No.1 and H-No.1H are approximately 0.31% and those of N-No.2 and H-No.2 are approximately 0.46%. On the other hand, high strength upper reinforcements in the proposed beams, i.e., H-No.1 and H-No.2, yielded at drifts more than 2.0%, in particular, H-No.1 have maintained elasticity of upper reinforcement and the second stiffness k_2 until large drift. This is considered to be led by the contraflexure point shifting near to the left beam end (see Fig.4(c)) than that of H-No.2 as a result of reducing to two reinforcements to four upper reinforcements at beam ends. The stiffness ratios of k_2 to k_1, i.e., α defined in Fig.3, were 21% for H-No.1 and was 22% for H-No.2.

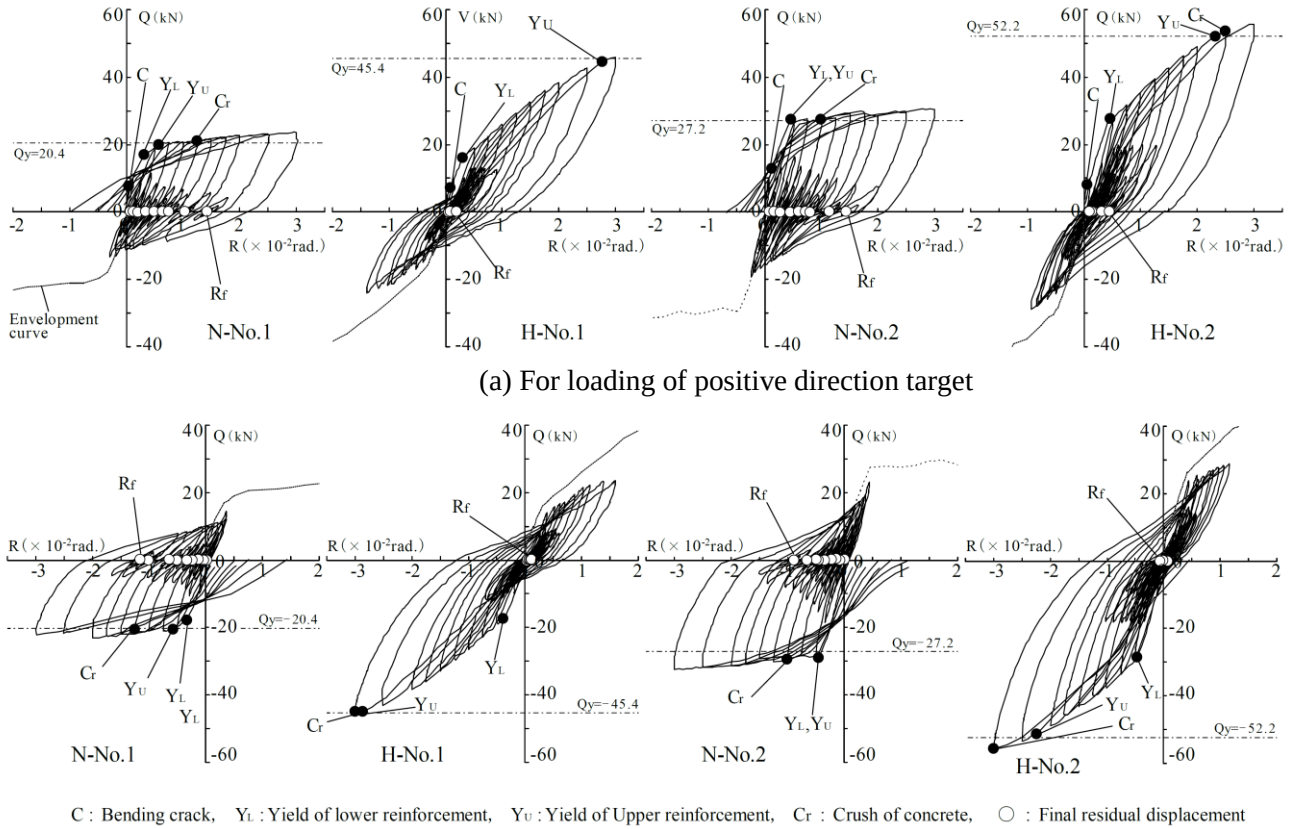

(a) For loading of positive direction target

(b) For loading of negative direction target

Fig. 18 –Hystreisis loops of vertical shear force and drift curves and hysteresis loops of beams

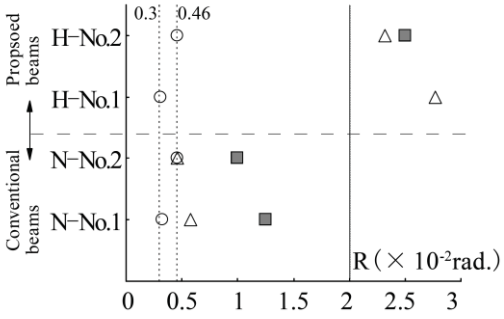

Fig. 19— Dsipacement drift at yield of rebars and crush of concrete under positive loading direction

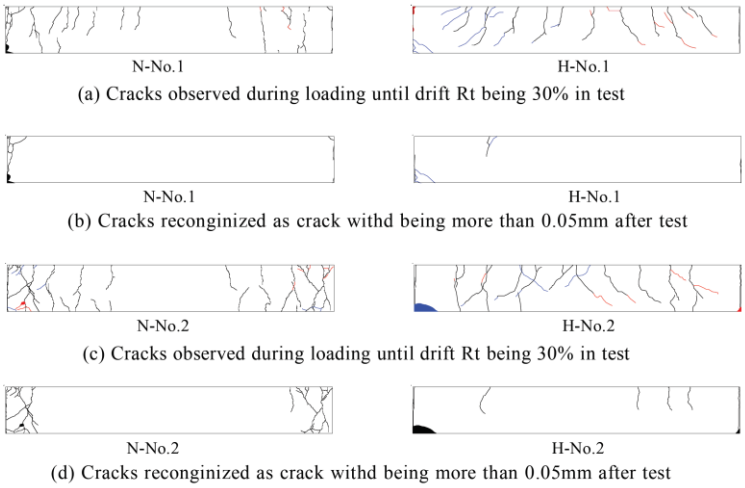

Fig. 20—Creacks obseved during laoding and recongnized as cruck width being more than 0.05mm after test

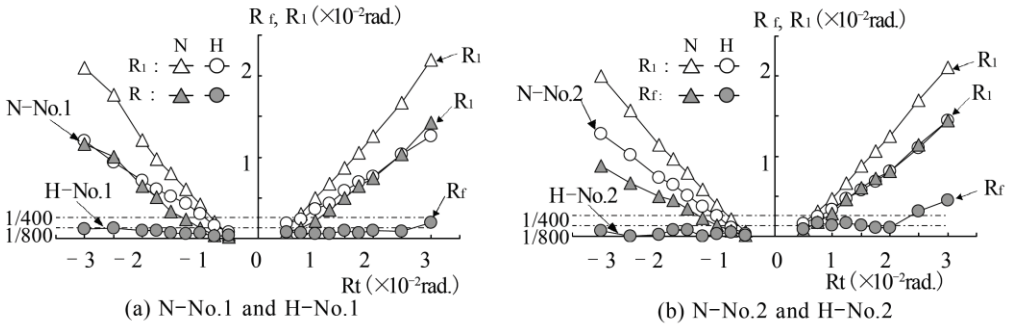

Fig. 21—Final residual displacement drift as target drift Rt increasing

3.3.2 Control of low damage

Fig. 20 shows sketched cracks and crushing observed until drift=30% and cracks more than 0.05mm in crack width after loading tests. In H-No.1and H-No.2, most of cracks more than the 0.05mm did not occurred until drift=20%. Most cracks in the proposed beam specimens, H-No.1and H- No.2, were observed to close gradually as rocking during the free-vibration loading. This phenomenon was not observed in the control specimens. The crushing of concrete in the proposed beam specimens was observed at drifts more than 50%. In H-No.1, the crushing was observed at negative drift=30%.

3.3.3 Final residual displacement

Fig.21 shows relationship of the final residual drift and the target displacement drift under free-vibration loading: R_f represents the final drift and R_1 is the first drift at shear force being zero immediately after unloading from the target displacement (see Fig.17). The horizontal dashed line indicates the drift 1/400 of threshold whether most people can or not recognize, in visual, the decline of a line. The proposed beam specimens suppressed their residual drifts less than 1/400; in particular, H-No.1 suppressed less than 1/800 and produced extremely excellent re-centring performance.

4. Summary

This paper proposed reinforcement arrangement for beam of cast-in-place reinforced concrete frame in order to produce high re-cenetring performance of frame, based on the concept of the vibration-control structure. Also, this paper reported detail of the reinforcement of beam, the mechanism of the re-cenering, and an experimental loading test of beams for verification of the concept.

The results from the experimental test demonstrated potential of the concept as followings:

i: Replacing all upper reinforcement in beam by high-strength can suppress its residual displacement drift after earthquake to be less than 1/400, without post-tensioning: moreover reducing half of lower reinforcement amount can suppress the drift to be less than 1/800.

ii: Most of bending cracks also closed in crack width to be negligible as the magnitude of suppressing the residual displacement boosts.

We have already conducted dynamic vibration analysis with earthquake motions for multi-storey frame adopting the proposed beam and confirmed the beam's effectiveness on suppressing the residual displacement and deflection at mid-span of the beam after the earthquakes[9].

5. Acknowledgements

This research has been funded by Japan Society for the Promotion of Science, 2013-2015

6. References

[1] Priestley M.J.N. (1991): Overview of PRESSS research program. *Earthquake Engineering & Structural Dynamics*, **31** (3), 491-514.

[2] Priestley, N., Sritharan, S., Conley, J., and Pampanin, S. (1999): Preliminary Results and Conclusions From the PRESSS Five-Story Precast Concrete Test Building. PCI Journal (Nov-Dec 1999), 42-67

[3] Priestley M.J.N., Calvi G.M., and Kowalsky M.J. (2007): Displacement-based seismic design of structures. IUSS Press.

[4] Daniela Wrzesniak, Geoffrey W. Rodgers, Massimo Fragiacomo, J. Geoffrey Chase (2014): Damage avoidance desing of timber structures using high-force-volume damping devices. World Conference on Timber Engineering WCTE2014, Quebec City, Canada, 2014

[5] Felice Carlo Ponzo, Antonio Di Cesare, Domenico Nigro, Michele Simonetti, Tobias Smith, Stefano Pampanin (2014): Shaking table testing of a multi-storey posttensioned glulam building: preliminary experimental results. World Conference on Timber Engineering WCTE2014, Quebec City, Canada, 2014

[6] Tom Armstrong1,Tobias Smith, Andrew H. Buchanan (2014): Seismic detailing of post-tensioned timber frames. World Conference on Timber Engineering WCTE2014, Quebec City, Canada, 2014

[7] Francesco Sarti, Alessandro Palermo, Stefano Pampanin (2014): Design and testing of post-tensioned timber wall systems. World Conference on Timber Engineering WCTE2014, Quebec City, Canada, 2014

[8] Zarnani, P., Valadbeigi, A., and Quenneville, P. (2016): Resilient slip friction (RSF) joint: A novel connection system for seismic damage avoidance design of structures. World Conference on Timber Engineering WCTE2016, Vienna Univ. of Technology, Vienna, Austria.

[9] Atsuya, K. Shinichi, S (2018): Time History Response Analysis of Reinforced Concrete Frames Inducing Self-centering, Proceedings of the Japan Concrete Institute, JCI Annual Convention in KOBE p.p.752-756 (in Japanese)

